Assessing the capability of the Wilshire equations in predicting uniaxial creep curves: an application to Waspaloy

Mark Evans[1*], Tom Williams[2]

[1]College of Engineering, Swansea University, Fabian Way, Crymlyn Burrows, Wales, SA1 8EN, UK; m.evans@swansea.ac.uk; Tel.: 01792295748. Corresponding author.*

[2]Institute of Materials, Bay Campus, Swansea University, Swansea SA1 8EN, UK; 825982@swansea.ac.uk.

ABSTRACT: It is important to be able to predict creep strains in aeroengine so as to enable small punch disc test results to be related to uniaxial creep test results using finite element models. The capability of the Wilshire equation to interpolate creep curves was assessed using creep tests on Waspaloy. This assessment required modifying the Wilshire equation for time to strains so that the parameters of this equation could be predicted as a function of strain in a way that did not allow predicted creep curves to double back on themselves. An artificial neural network was used to achieve this. It was found that the modified model was capable of interpolating the shape and the end points of the experimental creep curves. These modifications enabled the activation energy to be measured and it was found that the activation energy is dependent upon the average internal stress and thus strain.

Keywords: Creep curves, Wilshire equations, Interpolative evaluation, ANN

1. Introduction

Since the 1950s, the introduction of new materials have supported major improvements in the power, efficiency and reliability of aeroengines, underpinning impressive advances in the performance and safety of aircraft [1]. However recent escalating energy prices, growing environmental concerns, and the rising demand for travel, are requiring further increases in engine efficiency to minimise fuel consumption and greenhouse gas emissions. However, achieving greater efficiencies through higher operating temperatures requires materials with enhanced temperature capabilities and the nickel based superalloy, Waspaloy, is an example of one such material. Unfortunately, the 'materials development cycle' from concept to application currently takes many years [2]. In particular, long duration test programmes are needed to establish the tensile stresses which can be sustained over the planned design lives without creep failure occurring at the temperatures encountered during service.

In order to prevent aeroengine blades rubbing against the engines outer casing, strain is a very important design and material development criteria. Being able to realistically predict strain at given times is also very important for converting small punch test data into equivalent uniaxial test results given that the most promising way of doing this is via finite element models of the punch test, These finite element models require equations for working out incremental increases in strain with time and so require accurate predictions of all points along a creep curve. The successful correlation of small punch and uniaxial test results will help release the full potential of the small punch test. The Wilshire equations have shown great potential in reducing the length of the development cycle because it has been shown in the literature to produce reliable failure time and minimum creep rate predictions for operating conditions (or close to) from very short term accelerated tests [3-12]. However, this literature is quite sparse on how to modify the Wilshire equations so as to be able to predict times to specified strains and therefore complete creep curves [13-14]. Given the importance of strain for developing new aeroengine materials, the aim of this paper is to I. in a novel way rework the existing Wilshire equations, so that whole creep curves can be predicted at any test condition within the experimental range of test conditions and ii. introduce various performance statistics that can be used to evaluate the interpolated creep curves. A final aim of this paper is to highlight the different creep regimes working within the data set used in this paper, a phenomenon that the original investigators of this data set failed to identify -Wilshire and Scharning [16]

To achieve this objective the paper is structured as follows. The next section describes the creep tests of the polycrystalline nickel alloy Waspaloy that have been conducted at Swansea University. Section 3 reviews the Wilshire equations as applied to minimum creep rates, failure times and times to various strains. The role on the Monkman – Grant relation in tying all these equations together is explained, together with the few attempts that have been made to amend the Wilshire equation to enable interpolation/extrapolation of complete creep curves. In section 4, criteria are outlined for assessing how good the creep curve predictions are, with all these techniques then being applied to Waspaloy in section 5. The paper concludes by outlining some suggestions for future research.

2. The data

Thirty cylindrical test pieces were machined from the as received Waspaloy bar, with a gauge length of 25.4mm and a diameter of 4mm. The chemical composition of this batch of Waspaloy (in wt. %) was determined to be within the compositional limits for Waspaloy - 18–21Cr, 12–15Co, 3.5–5Mo, 2.75–3.25Ti, 1.2–1.6Al, 0.02–0.1C and 0.003–0.01B, balance Ni

(wt.%). These test pieces were solution treated at 1315 K (4 h), stabilised at 1115 K (4 h) and aged at 1030 K (16 h), with the samples air cooled between each heat treatment stage. The tensile strength (σ_{TS}) values for this batch of materials were 1154, 1120, 975 and 827 MPa at 873, 923, 973 and 1023 K respectively.

Thirty specimens were tested in tension over a range of stresses at 873K, 923K, 973K and 1023K using high precision constant-stress machines described elsewhere [15]. At 873K, seven specimens were placed on test over the stress range 1050 MPa to 700 MPa, at 923K seven specimens were placed on test over the stress range 1000 MPa to 550 MPa, at 973K nine specimens were placed on test over the stress range 950 MPa to 200MPa and at 1023K seven specimens were tested over the stress range 700 MPa to250 MPa. Up to 400 creep strain/time readings were taken during each of these tests. Because Waspaloy can serve at temperatures up to 920 K for critical applications and 1040 K for less demanding situations, the test programme covered stress ranges giving creep lives up to 5500 h (around 19852000 s) at 873 to 1023 K. This data set was first published by Wilshire and Scharning [16]. However, in their analysis they considered only part of their data set and so failed to identify the different creep regimes actually present in this material. They also limited their analysis to failure times (time to rupture strain) and did not consider times to other strains

3. Review of the Wilshire equations

In the initial published article describing the Wilshire methodology [3], three equations were postulated to describe the behaviour of the minimum creep rate, times to failure and times to any strain.

3.1. The minimum creep rate

Since the first appearance of the Wilshire equations in the engineering literature, the exact form of these equations has evolved to cope with the different properties of the high temperature materials to which they have been applied. The following representation of the Wilshire equation for the minimum creep rate, $\dot{\varepsilon}_m$, captures most of this evolution

$$\sigma/\sigma_{TS} = \exp\left\{-k_{2j}\left[\dot{\varepsilon}_m \exp\left(Q^*_{cj}/RT\right)\right]^{v_j}\right\}$$
$$j = 1 \text{ when } \sigma/\sigma_{TS} \le \sigma_1^c;\ \ j = 2 \text{ when } \sigma_1^c < \sigma/\sigma_{TS} \le \sigma_2^c;\ \ \ldots;\ j = p \text{ when } \sigma/\sigma_{TS} > \sigma_p^c \qquad (1a)$$
$$\sigma_1^c < \sigma_2^c < \ldots\ldots\ldots < \sigma_p^c$$

where T is the absolute temperature, σ the stress, σ_{TS} the tensile strength, R the universal gas constant, Q^*_{cj} the activation energies for $\dot{\varepsilon}_m$ in each of the p normalised stress ranges and k_{2j} and v_j are further model parameters that require estimation. σ^c_j are critical values for the normalised stress and so fall between 0 and 1. In this approach, there are p creep regimes that occur in distinct ranges for the normalised stress and the p versions of Eq. (1a) then apply to each regime. Typical, p varies between 1 and 4 depending on the material being studied. Some of the first studies to appear in the literature include applications to Copper [3] and 1Cr-1Mo-0.25 steel [4] where p was found to equal 2 and where the activation energy was the same either side of σ_1^c (so $Q^*_{cj} = Q^*_c$). Latter studies by Whittaker and Wilshire using 2.25Cr-1Mo steel [5] found p to equal 3 and again the activation energy was the same either side of σ_1^c and σ_2^c, Evans [6] found p = 2 but with a varying activation energy either side of σ_1^c when studying a 12Cr steel. Wilshire et. al. found similar results in their application to 316 stainless steel [8]. Finally,

Whittaker et. al. [9] found p = 2 with varying activation energies around σ_1^c when studying a particular grade of Waspaloy.

For estimation purposes, and making use of the natural logarithmic transformation ln[], Eq. (1) can be rewritten as

$$\ln[\dot{\varepsilon}_m] = a_{0j} + a_{1j}\ln[-\ln(\sigma/\sigma_{TS})]+a_{2j}\,[1/RT] \quad ; \quad j = \text{to } p \tag{1b}$$

where $v_j = 1/a_{1j}$, $k_{2j} = \exp(-a_{0j}/a_{1j})$ and $Q^*_{cj} = -a_{2j}$. In this format, and with p = 1, the parameters a_{01} to a_{21} can be estimated using the least squares technique through a regression of $\ln[\dot{\varepsilon}_m]$ on $\ln[-\ln(\sigma/\sigma_{TS})]$ and 1/RT. When p = 2, estimation requires the construction of two new variables by initially estimating (by eye) a value for σ_1^c

$$\ln[\dot{\varepsilon}_m] = a_0 + a_1\ln[-\ln(\sigma/\sigma_{TS})]+a_2\,[1/RT] + a_3 Max(0, \sigma^*)+a_4\,[D/RT] \tag{1c}$$

where $\sigma^* = \ln[-\ln(\sigma/\sigma_{TS})] - \ln[-\ln(\sigma_1^c)]$, D = 0 when $\sigma^* \le 0$ and D = 1 when $\sigma^* > 0$. When j = 1 and so $\sigma^* \le 0$, Eq. (1c) collapses to

$$\ln[\dot{\varepsilon}_m] = a_0 + a_1\ln[-\ln(\sigma/\sigma_{TS})]+a_2\,[1/RT]$$

and so $a_{01} = a_0$, $a_{11} = a_1$ and $a_{21} = a_2$. Thus $v_1 = 1/a_1$, $k_{21} = \exp(-a_0/a_1)$ and $Q^*_{c1} = -a_2$. Then when j = 2 and so $\sigma^* > 0$ with D = 1, Eq. (1c) can be re-arranged as

$$\ln[\dot{\varepsilon}_m] = \{a_0 - a_3\ln[-\ln(\sigma^*)]\} + (a_1 + a_3)\ln[-\ln(\sigma/\sigma_{TS})]+ (a_2 + a_4)\,[1/RT] \tag{1d}$$

and so $a_{02} = a_0 - a_3\ln[-\ln(\sigma^*)]$, $a_{12} = a_1 + a_3$ and $a_{22} = a_2 + a_4$. Thus $v_2 = 1/a_{12}$, $k_{22} = \exp(-a_{02}/a_{12})$ and $Q^*_{c2} = -a_{22}$. All these parameters are estimated by a regression of $\ln[\dot{\varepsilon}_m]$ on $\ln[-\ln(\sigma/\sigma_{TS})]$, 1/RT, $Max(0, \sigma^*)$ and D/RT. This regression will have an associated coefficient of determination (R^2) - that shows what percentage of the variation in $\ln[\dot{\varepsilon}_m]$ that can be explained by variations in all the variables on the right hand side of Eq. (1c). This regression is carried out for all values of σ_1^c within the experimental range of normalised stresses and the value σ_1^c is that value which gives the largest R^2 value.

3.2. The time to failure

The above Wilshire equation for the minimum creep rate is the fundamental relationship from which all the others should be derivable. Thus, the second Wilshire equation, for the time to failure t_f, has traditionally been written as

$$\sigma/\sigma_{TS} = \exp\left\{-k_{1j}\left[t_f \exp\left(-Q^*_{cj}/RT\right)\right]^{u_j}\right\} \quad ; \quad j = 1 \text{ to } p \tag{2a}$$

and k_{1j} and u_j are additional model parameters that require estimation. In fact, k_{1j} and u_j can be linked back to k_{2j} and v_j in a number of ways. The simplest possibility is through the Monkman -Grant [17] relation of the form

$$\dot{\varepsilon}_m = M/t_f \tag{2b}$$

so that $u_j = -v_j$ and $k_{1j} = k_{2j}M^{vj}$. For many high temperature materials however, the exponent on $\dot{\varepsilon}_m$ is not unity, so that more generally

$$[\dot{\varepsilon}_m]^{\rho} = M/t_f \qquad (2c)$$

Substituting Eq.(2c) into Eq. (1b) then yields

$$\sigma/\sigma_{TS} = \exp\left\{-k_{1j}\left[t_f \exp\left(-Q_{cj}^{**}/RT\right)\right]^{u_j}\right\} \quad ; \quad j = 1 \text{ to } p \qquad (2d)$$

with the restrictions $u_j = -v_j/\rho$, $k_{1j} = k_{2j}M^{vj/\rho}$ and $Q_{cj}^{**} = \rho Q_{cj}^{*}$.

Dunand et. al. [18], when looking at dispersion strengthened and particulate reinforced Aluminium, noted that a better fit to the experimental data was obtained by introducing the strain at failure ε_f into Eq. (2c)

$$[\dot{\varepsilon}_m]^{\rho^*} = C[\varepsilon_f/t_f] \qquad (2e)$$

Substituting Eq. (2e) into Eq. (1b) then yields

$$\sigma/\sigma_{TS} = \exp\left\{-k_{4j}\left[t_f/\varepsilon_f \exp\left(-Q_{cj}^{**}/RT\right)\right]^{u_j}\right\} \quad ; \quad j = 1 \text{ to } p \qquad (2f)$$

with $u_j = -v_j/\rho^*$, $k_{4j} = k_{2j}C^{vj/\rho^*}$ and $Q_{cj}^{**} = \rho^* Q_{cj}^{*}$.

For estimation purposes, Eq. (2d) or Eq. (2f) can be rewritten as

$$\ln[t_f] = b_{0j} + b_{1j}\ln[-\ln(\sigma/\sigma_{TS})] + b_{2j}[1/RT] \quad ; \quad j = 1 \text{ to } p \qquad (2g)$$

with $u_j = 1/b_{1j}$, $k_{1j} = \exp(-b_{0j}/b_{1j})$ and $Q_{cj}^{**} = b_{2j}$ or

$$\ln[t_f] - \ln[\varepsilon_f] = c_{0j} + c_{1j}\ln[-\ln(\sigma/\sigma_{TS})] + c_{2j}[1/RT] \quad ; \quad j = 1 \text{ to } p \qquad (2h)$$

-with $u_j = 1/c_{1j}$, $k_{4j} = \exp(-c_{0j}/c_{1j})$ and $Q_{cj}^{**} = c_{2j}$

In these formats, the parameters b_{0j} to b_{2j} and c_{0j} to c_{2j} can be estimated using the least squares technique through a regression of $\ln[t_f]$ on $\ln[-\ln(\sigma/\sigma_{TS})]$ and $1/RT$ or $\ln[t_f] - \ln[\varepsilon_f]$ on $\ln[-\ln(\sigma/\sigma_{TS})]$ and $1/RT$. A break can be allowed for in exactly the same way as in the previous sub section:

$$\ln[t_f] = b_0 + b_1\ln[-\ln(\sigma/\sigma_{TS})] + b_2[1/RT] + b_3 \text{Max}(0, \sigma^*) + b_4[D/RT] \qquad (2i)$$

or

$$\ln[t_f] - \ln[\varepsilon_f] = c_0 + c_1\ln[-\ln(\sigma/\sigma_{TS})] + c_2[1/RT] + c_3 \text{Max}(0, \sigma^*) + c_4[D/RT] \qquad (2j)$$

3.3. The time to strain

The final Wilshire equation is

$$\sigma/\sigma_{TS} = \exp\left\{-k_{3j}\left[t_{\varepsilon}\exp\left(-Q_{cj}^{***}/RT\right)\right]^{w_j}\right\} \quad ; \quad j = 1 \text{ to } p \tag{3a}$$

where t_ε is the time taken to reach strain ε and k_{3j} and w_j are model parameters that require estimation. Compared to the Wilshire failure time and minimum creep rate equations there is however one additional complication that occurs because at some of the strain values some specimens will have already failed and so there will be no corresponding t_ε value for these test specimens. This leads to the unsatisfactory result that the number of specimens used for parameter estimation purposes will vary with ε. One solution is to normalise the strain by dividing it through by the failure strain ε_f so that for every specimen $\varepsilon^* = \varepsilon/\varepsilon_f$ varies between 0 and 1 as t_{ε^*} varies between 0 and t_f

$$\sigma/\sigma_{TS} = \exp\left\{-k_{3j}^{*}\left[t_{\varepsilon^*}\exp\left(-Q_{cj}^{***}/RT\right)\right]^{w_j^{*}}\right\} \quad ; \quad j = 1 \text{ to } p \tag{3b}$$

Then for estimation purposes, Eq. (3b) can be rewritten as

$$\ln[t_{\varepsilon^*}] = d_{0j} + d_{1j}\ln[-\ln(\sigma/\sigma_{TS})] + d_{2j}[1/RT] \quad ; \quad j = 1 \text{ to } p \tag{3c}$$

with $w^*_j = 1/d_{1j}$, $k^*_{3j} = \exp(-d_{0j}/d_{1j})$ and $Q_{cj}^{***} = d_{2j}$. In this format, the parameters d_{0j} to d_{2j} can be estimated using the least squares technique through a regression of $\ln[t_{\varepsilon^*}]$ on $\ln[-\ln(\sigma/\sigma_{TS})]$ and $1/RT$. A break can be allowed for in exactly the same way as in the previous sub sections:

$$\ln[t_{\varepsilon^*}] = d_0 + d_1\ln[-\ln(\sigma/\sigma_{TS})] + d_2[1/RT] + d_3 \text{Max}(0, \sigma^*) + d_4[D/RT] \tag{3d}$$

For Eq. (3b) and Eq. (2a) to be consistent, the parameters k^*_{3j} and w^*_j must vary with strain in such a way that as $\varepsilon^* \to 1$ (and so as $\varepsilon \to \varepsilon_f$) then $k^*_{3j} \to k_{1j}$ and $w_j \to u_j$. This implies that f_{1j} and f_{2j} in Eq. (3e) below are functions containing strain, the exact form of which was never specified in the original Wilshire methodology

$$w^*_j = f_{1j}(\varepsilon^*) \text{ and } \quad k^*_{3j} = f_{2j}(\varepsilon^*) \tag{3e}$$

This allows the prediction of times to reach given normalised strains and so the prediction of whole (partially normalised) creep curves at any stated stress and temperature using

$$t_{\varepsilon^*} = -\frac{[\ln(\sigma/\sigma_{TS})/f_{2j}(\varepsilon^*)]^{1/f_{1j}(\varepsilon^*)}}{\exp\left(-Q_{cj}^{***}/RT\right)} \tag{3f}$$

When it comes to predicting the creep curves at stresses and temperatures different from those in the experimental data set (interpolation or extrapolation), ε_f will of course not be known. One approach would then be to use Eq. (2e), (whose parameters are estimated from the experimental test data), and substitute into this equation the predicted minimum creep rates and failure times obtained from the Wilshire equations for these variables [Eqs. (1c,2i)] and finally solving for ε_f. As an alternative, use can be made of Eqs. (2i,2j), (whose parameters are estimated from the experimental test data), to predict $\ln[t_f]$ and $\ln[t_f] - \ln[\varepsilon_f]$ separately and from these two predictions a prediction of $\ln[\varepsilon_f]$ can be obtained.

Eqs. (1a,2a) have been applied to numerous high temperature materials partly because there are extensive creep data bases in the public domain that contain failure times and minimum

creep rates. The National Institute for Materials Science (NIMS) in Japan [19] have published numerous creep date sheets (one for each material) showing times to failure and minimum creep rates at various temperatures and constant loads. Similar data sets exist in Europe as published by the European Creep Collaborative Committee (ECCC) [20] and in the UK as published by British Steelmakers Creep Committee (BSCC) [21]. However, Eq. (3a) has been applied in just a few instances because these public domain data bases do not contain whole creep curves (at best they have times taken to reach a few very low strains). The few exceptions include a study by Abdallah et. al. [13] who assumed the w_{3j} were fixed with respect to strain when using this approach to predict creep curves for Titanium (but strangely did not specify a form for $f_{2j}(\varepsilon)$). Harrison et. al. [12], when studying Nickel based super alloys, again assumed w_{3j} to be fixed but with

$$k_{3j} = k_{3j,0} + k_{3j,1}\varepsilon^{-k_{3j,2}} \tag{4}$$

The problem with Eq. (4]) is that it does not ensure $k_{3j} \to k_{1j}$ as $\varepsilon \to \varepsilon_f$. More recently, Gray and Whittaker [14] when studying Waspaloy proposed a model for predicted creep curves that appeared to bypass the Wilshire methodology altogether by working with

$$t_\varepsilon = M(\varepsilon)\frac{\left(1 - \frac{\sigma}{\sigma_{TS}}\right)^{P(\varepsilon)}}{\exp\left(-Q_c^{***}/RT\right)} \tag{5a}$$

where M and P are parameters whose value depends in some way of the strain ε. Whilst Eq. (5a) is similar to Eq. (3f) it does not have the Wilshire equations as its bases because although it uses the normalised stress it does not taking the double logarithmic transformation of this normalised stress. The authors also observed a complicated relationship between P and ε and also between M and ε which they modelled using

$$M(\varepsilon) = A_1 \exp\left(-\left(\varepsilon/A_2\right)^{-A_3}\right) \tag{5b}$$

$$P(\varepsilon) = A_7 + \frac{A_4}{\varepsilon A_5\sqrt{2\pi}}\exp\left(-\ln\left(\frac{A_6\varepsilon}{2A_5^2}\right)^2\right) \tag{5c}$$

where A_1 to A_7 are model parameters that require estimation. The parameters in Eqs. (5b,c) are quite difficult to estimate as they require the use of non linear optimisation procedures. Further, they are not consistent with the Wilshire time to failure equation in that there is not guarantee that as ε tends to the rupture strain, these equations will produce values for k_{3j} and w_j that tend to k_{1j} and u_j. As result it is possible for these equation to predict creep curve shapes that double back on themselves at high strains.

Therefore, in this paper a different approach is used that is i. much more flexible than Eqs. (5b,c) and so should enable better predictions to be made, ii.is such that k_{3j} and w_j tend to k_{1j} and u_j as strain approach the rupture strain (and so avoids the issue of doubling back) and iii. only requires simple linear optimisation procedures – such as linear least squares. The empirical approach adopted for this paper is an Artificial Neural Network (ANN) which is used to represent the functional forms in Eq. (3e), so that the Wilshire approach in Eq. (3f) can then be used to model the creep curve. Following Martin et. al. [22] this ANN is specified as

$$w_j^* = \phi_{0j} + \phi_{1j}\varepsilon^* + \sum_{i=1}^{m} \beta_{ij}\left[\frac{1}{1+\exp(\delta_{0ij}+\delta_{1ij}\varepsilon^*)}\right] \qquad j = 1 \text{ to } p \qquad (6a)$$

$$k_{3j}^* = \phi_{2j} + \phi_{3j}\varepsilon^* + \sum_{i=1}^{m} \lambda_{ij}\left[\frac{1}{1+\exp(\delta_{2ij}+\delta_{3ij}\varepsilon^*)}\right] \qquad j = 1 \text{ to } p \qquad (6b)$$

It is also possible that the Q^{***}_{cj} also varies with the normalised strain. For example, Davies [23] first suggested that the activation energy is only constant during steady state creep where a dynamic equilibrium rate occurs. Outside steady state creep he proposed that the activation energy would be dependent upon the average internal stress. Further, Estrin and Mecking [24] showed that the evolution of the internal stress can be derived from the evolution of the dislocation density as a function of the creep strain (via a first order partial differential equation)) so that the activation is also a function of strain. More precisely they showed that the activation energy is modified exponentially function of strain such that as strain increases the activation energy tends to that associated with steady state creep. To allow for this type of variation, Q^{***}_{cj} can aso be given an ANN representation

$$Q_{cj}^{***} = \phi_{4j} + \phi_{5j}\varepsilon^* + \sum_{i=1}^{m} \gamma_{ij}\left[\frac{1}{1+\exp(\delta_{4ij}+\delta_{5ij}\varepsilon^*)}\right] \qquad j = 1 \text{ to } p \qquad (6c)$$

To estimate the unknown parameters of Eqs. (6a,b), m is first fixed at one, and values for all the δ parameters are guessed at enabling the expressions in parenthesis to be converted into variables. For Eq. (6a) a regression of w_{*j} on ε^* and $\frac{1}{1+\exp(\delta_{0i}+\delta_{1i}\varepsilon^*)}$ can then be carried out. This regression will have an associated coefficient of determination (R^2). This regression is carried out for values of δ_{01} and δ_{11} within a defined 2x2 grid of values for δ_{01} and δ_{11} and the values δ_{01} and δ_{11} are taken to be those values which gives the largest R^2 value . Once R^2 is maximised, R^2_{max}, the following Akaike Information Criteria [25] criteria is used to choose the value for m

$$AIC = S[1-R^2_{max}]\exp[2(3m+2)/n] \qquad (6d)$$

where n is the number of test specimens and S is the standard deviation in w^*_j (or k^*_{3j} when using Eq. (6b)). This is used to prevent over fitting the data (i.e. achieving higher and higher R^2_{max} values) simply by choosing large values for m and so this criteria is useful for identifying more parsimonious models.

4. Evaluation

Very few publications on the Wilshire methodology have offered a rigorous assessment of how accurate the approach is, as they have tended to rely on visual plots of predictions alongside actual experimental results. The second aim of this paper is to remedy this, by suggesting the use of some powerful performance statistics that are in common use in the field of economic. The mean squared prediction error (MSPE) is often the starting point for the evaluation of any predictions made from a particular model. Letting y^a_i be the experimental (or actual) value for a creep property (such as time to failure, time to strain or minimum creep rate) obtained at the ith test condition (such as at σ = 700 MPa and T = 973K) and y^p_i the prediction made for that creep property, then the MSPE is given by

$$\text{MSPE} = \frac{\sum_{i=1}^{n}\left(y_i^a - y_i^p\right)^2}{n} \tag{7a}$$

where there are n creep specimens tested at n different test conditions. Whilst the squaring of the prediction error prevents under predictions being offset by over predictions in the averaging procedure, the MSPE provides not sense of scale for the prediction errors. One simple modification of Eq. (7a) that introduces a sense of scale is to replace y^a and y^p with the natural log of their values. This scaling comes about because when using the natural logs of the creep properties and their predictions, the MSPE associated with the logged data is approximately equal to the mean percentage square error (MPSE) associated with the raw (untransformed) data:

$$\frac{\sum_{i=1}^{n}\left(\ln[y_i^a] - \ln[y_i^p]\right)^2}{n} \cong \text{MPSE} = \frac{\sum_{i=1}^{n}\left([y_i^a - y_i^p]/y_i^p\right)^2}{n} \tag{7b}$$

with this approximation being better the smaller are the percentage errors. This MPSE can be decomposed in one of two ways. Theil [26] has shown that

$$\text{MPSE} = \left(\overline{\ln[y^a]} - \overline{\ln[y^b]}\right)^2 + \text{Var}\left(\ln[y_i^a] - \ln[y_i^p]\right) = \left(\overline{\ln[y^a]} - \overline{\ln[y^b]}\right)^2$$

$$+\left(\sigma^a - \sigma^b\right)^2 + 2(1\text{-}r)\sigma^a\sigma^b \tag{7c}$$

where $\overline{\ln[y^a]}$ is the mean of the variable $\ln[y^a{}_i]$ (called the log mean), $\overline{\ln[y^b]}$ is the mean of the variable $\ln[y^b{}_i]$, σ^a is the standard deviation for the variable $\ln[y^a{}_i]$, σ^p is the standard deviation for the variable $\ln[y^p{}_i]$, and r is the correlation coefficient between $\ln[y^a{}_i]$ and $\ln[y^b{}_i]$. $\text{Var}\left(\ln[y_i^a] - \ln[y_i^p]\right)$ reads the variance of the percentage prediction error $(y_i^a - y_i^p)/y_i^p$. Dividing both sides by the MPSE defines what Theil called the proportions of inequality

$$1 = \frac{\left(\overline{\ln[y^a]} - \overline{\ln[y^b]}\right)^2}{\text{MPSE}} + \frac{\left(\sigma^a - \sigma^b\right)^2}{\text{MPSE}} + \frac{2(1\text{-}r)\sigma^a\sigma^b}{\text{MPSE}} = U^M + U^S + U^C \tag{7d}$$

The bias proportion U^M is an indication of systematic error since it measures the extent to which the average values of the predicted and actual logged series deviate from each other. It is a systematic error because the average creep property is determined by the average test conditions that generated the $y^a{}_i$ series. The variance proportion U^S indicates the ability of the creep model to replicate the extent to which actual and predicted log creep properties deviate from their log mean values as a result of changes in test conditions. Therefore, this is also systematic error. The covariance proportion U^C measures random or unsystematic error and represents the remaining prediction error after deviations from average values have been accounted for. Experimental errors associated with measuring creep properties, means that it is unreasonable to expect the predictions made from any model to be perfectly correlated with actual values and so this component is less of a concern than the other two.

To make it easier to compare the accuracy of various creep models, the MPSE is often re-scaled to be within the range zero to one as follows

$$U = \frac{\sqrt{\frac{\sum_{i=1}^{n}\left(\ln[y_i^a] - \ln[y_i^p]\right)^2}{n}}}{\sqrt{\frac{1}{n}\sum_{i=1}^{n}\left(\ln[y_i^a]\right)^2} + \sqrt{\frac{1}{n}\sum_{i=1}^{n}\left(\ln[y_i^p]\right)^2}} \quad (7e)$$

The numerator of U is the square root of the MPSE and is often called the root mean percentage square error or RMPSE. The denominator scales U to fall between 0 and 1 (in much the same way as the scaling used to convert the covariance to a correlation coefficient). If U = 0, then $y^a_i = y^b_i$ for all i (i.e. over all the different test conditions) and the model is a perfect predictor of the creep properties under analysis. If U = 1, the predictive performance of the creep model is as bad as it could possibly be. Hence U measures the RMPSE in relative terms.

Peel et. al. [27] proposed an alternative decomposition based around a plot of the actual (but in logs) creep property series against a series made up of the models predictions, namely

$$\ln[y_i^a] = \alpha_0 + \alpha_1 \ln[y_i^p] + e_i \quad (8a)$$

It follows from this equation that the percentage prediction error is (approximately) given by

$$\ln[y_i^a] - \ln[y_i^p] = \alpha_0 + (\alpha_1 - 1)\ln[y_i^p] + e_i \quad (8b)$$

and so

$$\mathrm{Var}(\ln[y_i^a] - \ln[y_i^p]) = (\alpha_1 - 1)^2(\sigma^b)^2 + \sigma_e^2 \quad (8c)$$

where σ^2_e is the variance of the residual term e_i. The least squares estimate of α_0 is also given by $\overline{\ln[y^a]} - \alpha_1 \overline{\ln[y^b]}$ and so $\left(\overline{\ln[y^a]} - \overline{\ln[y^b]}\right)^2 = (\alpha_0 + (\alpha_1 - 1)\overline{\ln[y^b]})^2$ allowing the MPSE to be decomposed as

$$\mathrm{MPSE} = (\alpha_0 + (\alpha_1 - 1)\overline{\ln[y^b]})^2 + (\alpha_1 - 1)^2(\sigma^b)^2 + \sigma_e^2 \quad (8d)$$

Therefore, part of the MPSE is attributable to the intercept (α_0) of the best fit line on a plot of $\ln[y^a_i]$ against $\ln[y^b_i]$ being different from zero and another part of the MPSE is attributable to slope (α_1) of the best fit line on a plot of $\ln[y^a_i]$ against $\ln[y^b_i]$ being different from 1. These parts of the MPSE are systematic in nature as they are caused by this best fit line being different from a 45 degree line on such a plot and so leads to either persistent under or over prediction of the y^a series. The remaining part of the MPSE is a random prediction error whose size is given by the variance of e or the extent to which the data are scattered around the best fit line on a plot of $\ln[y^a_i]$ against $\ln[y^b_i]$. Dividing both sides by the MPSE

$$1 = \frac{(\alpha + (\beta - 1)\overline{\ln[y^b]})^2}{MSE} + \frac{(\beta - 1)^2(\sigma^b)^2}{MSE} + \frac{\sigma_e^2}{MSE} = U^M + U^R + U^D \quad (8e)$$

By making some assumptions about the distribution for e in Eq. (8a), it is possible to further interpret σ_e. If e is assumed to be normally distributed with a mean of zero and standard deviation of σ_e, then $\frac{\sum_{i=1}^{n}([y_i^a - y_i^p]/y_i^p)}{n}$, or the mean percentage prediction error is equal to

$\exp(0.5\sigma^2_e) - 1$ (8f)

and the median percentage prediction error is equal to zero. The extent to which the value given by Eq. (8f) differs from $\frac{\sum_{i=1}^{n}([y_i^a - y_i^p]/y_i^p)}{n}$ can be taken as a measure of how valid this normality assumption is.

5. Application to Waspaloy data

5.1. The minimum creep rate

Using the method of estimation given in sub section 3A, Table 1a shows the parameter estimates of Eq. (1b)

Table 1a
Least Squares Estimates of the Parameters of Eq. (1b) with p = 2**.**

The p-value associated with a_4 in Eq. (1c)is 0.046%, suggesting that the activation energies above and below a normalised stress of 0.726 are significantly different from each other at the 1% significance level. Above a normalised stress of 0.726, the activation energy is approximately 223 kJ mol^{-1} and below this normalised stress it is 238 kJ mol^{-1}. Whilst this is not a big difference, it is never the less statistically significant. The p-value associated with a_3 is 7.27E-06% suggesting that the values for v above and below a normalised stress of 0.726 are significantly different from each other at the 1% significance level. This model is capable of explaining 96.30% of the variation observed in the logarithm of the minimum creep rates (as given by the coefficient of determination, R^2). Using the estimates in Table 1a and Eq (1d) above,

Below $\sigma_1^c = 0.726$: $v_2 = 1/a_{12} = 1/-5.328 = -0.189$, $k_{22} = \exp(-a_{02}/a_{12}) = \exp(-9.508/-5.328) = 5.958$ and $Q^*_{c2} = -a_{22} = 237{,}586$ J mol^{-1}:

$$\sigma/\sigma_{TS} = \exp\{-5.958[\dot{\varepsilon}_m \exp(237{,}586/RT)]^{-0.189}\} \quad (9a)$$

Above $\sigma_1^c = 0.726$: $v_1 = 1/a_{11} = 1/-1.413 = -0.708$, $k_{21} = \exp(-a_{01}/a_{11}) = \exp(-13.958/-1.413) = 19{,}495$ and $Q^*_{c1} = -a_{21} = 223{,}374$ J mol^{-1}:

$$\sigma/\sigma_{TS} = \exp\{-19{,}495[\dot{\varepsilon}_m \exp(223{,}374/RT)]^{-0.708}\} \quad (9b)$$

These activation energies are similar in value to that used by Wilshire et. al. [16] in his paper on this material, namely 276 kJ mol^{-1}. This activation energy pattern is the opposite to that observed by Whittaker et. al. [9] who observed higher activation energies at the higher stresses. Their interpretation was that the low activation energy was related to dislocation interaction with γ' precipitates below the yield stress. However, significantly increased dislocation densities at stresses above yield cause an increase in the activation energy values as forest hardening becomes the primary mechanism controlling dislocation movement. They proposed that this activation energy change is related to the stress increment provided by work hardening, as can be observed from Ti, Ni and steel results. The Waspaloy material used in this paper differed from that in the Whittaker et. al. [9] paper in both its chemical composition and heat treatment. The test conditions were also very different (the Whittaker et. al. [9] data had some higher temperatures and lower stresses). The process of deformation must therefore be

different between these materials. The observed activation energy change shown here is recall quite small in magnitude and this is consistent with the single activation energy found by Wilshire et. al. [16] when studying the same experimental data used in this paper.

This is all visualised in Fig. 1a where on the horizontal axis the minimum creep rates are temperature compensated using the estimated activation energies. The performance of the Wilshire equation is seen by the suitability of the best fit line that is kinked at the break point defined by a normalised stress of 0.726. Alternatively, in Fig.1b, $\ln[-\ln(\sigma/\sigma_{TS})]$ is plotted against the actual and the models predicted log minimum creep rate. The log of the minimum creep rate is shown so that the length of the error bars (shown as dashed bars in this figure) then corresponds to the percentage prediction error (divided by 100).

Table 1b further reveals that when these percentage errors are squared and then averaged, the Wilshire model predicts with MSPE of 45.61%, or with a root mean squared percentage error of 67.5%. This is put into further context by noting that Theil's U is 0.022, which is scaled to be within the range of 0 to 1, with zero corresponding to a model that produced perfect predictions. Based on Theil's decomposition of this MSPE, it is clear that nearly all of this percentage prediction error is random in nature (100%) so that the Wilshire model exhibits very little systematic error. This is further confirmed by Peel's decomposition where the p-values on α_0 and α_1 in Eq. (8a) reveal that α_0 is not significantly different from zero and α_1 is not significantly different from unity so that all the percentage prediction error is random in nature - whose magnitude is summarised in the standard deviation of e in Eq. (8a), σ_e = 0.700. Using Eq. (8f), $\exp(0.5\sigma^2_e)$ -1 = 27.76% which is an estimate of the mean percentage prediction error assuming normality of e (this is close to the actual mean percentage prediction error of 23.78%). What is important to realise is that this average percentage error produced by the Wilshire model is nearly all random in nature suggesting the model is not mis specified in any way and that this mean percentage error reflects the natural variation present in measuring the minimum creep rates from experimental creep curves (and so it is unlikely that this magnitude or error can be further reduced through use of any other creep model).

Fig. 1 - (a) Dependence of $\ln[\dot{\varepsilon}_m \exp(Q^*_c/RT)]$ on $\ln[-\ln(\sigma/\sigma_{TS})]$ at all temperatures; (b) Dependence of $\ln[\dot{\varepsilon}_m]$ on $\ln[-\ln(\sigma/\sigma_{TS})]$ with error bars equal to the % prediction error/100.

Table 1b
Summary of the predictive accuracy of Eq. (1b) using the parameter estimates shown in Table 1a.

5.2. The time to failure

Fig. 2a plots the minimum creep rate against the time to failure on a log scale, together with the best fit line. This best fit line explains nearly 97% of the variation in the log times to failure and provides a good fit at all the shown temperatures. So in Eq. (2c), M is estimated to be 1.557 and ρ to be -0.765. Further ,the p-value associated with the null hypothesis that ρ = -1 is 1.2E-07% and so it can be concluded that ρ differs from unity. Fig. 2b shows the version of the Monkman -Grant relation given by Eq. (2e) with C estimated at 4.386 and ρ^* at -0.854.

Fig. 2- (a) Dependence of $\ln[\dot{\varepsilon}]$ on $\ln[t_f]$ at all temperatures; (b) Dependence of $\ln[\dot{\varepsilon}_m]$ on $\ln[t_f] - \ln[\varepsilon_f]$.

Using the method of estimation given in sub section 3.2, Table 2a shows the parameter estimates of Eq. (2g):

Table 2a
Least squares estimates of the parameters of Eq. (2g**)**.

The p-value associated with b_4 is 0.092% suggesting that Q^{**}_c (and thus the activation energies) above and below a normalised stress of 0.726 are significantly different from each other at the 1% significance level. Above a normalised stress of 0.726, the activation energy (Q^*_c) is approximately $-b_{22}/\rho$ = -209/ -0.765 = 273kJ mol^{-1} and below the normalised stress it is $-b_{21}/\rho$ = -218/ -0.765 = 285 kJ mol^{-1}. These estimates are higher than those given in Table 1a based on using minimum creep rates rather than failure times, but are closer to the value of 276 kJ mol^{-1} used by Wilshire [16]. The p-value associated with b_3 is 1.56E-06% suggesting that the values for u above and below a normalised stress of 0.726 are significantly different from each other at the 1% significance level. This model is capable of explaining 97.20% of the variation observed in the logarithm of the times to failure (as given by the coefficient of determination, R^2). Using the estimates in Table 2a and Eq. (2g) above,

Below $\sigma_1^c = 0.726$: $u_2 = 1/b_{12} = 1/4.194 = 0.238$, $k_{12} = \exp(-b_{02}/b_{12}) = \exp(11.368/4.194) = 15.037$ and $Q^{**}_{c2} = b_{22} = 217{,}857$ J mol^{-1}:

$$\sigma/\sigma_{TS} = \exp\{15.037[t_f \exp(217{,}857/RT)]^{0.238}\} \quad (10a)$$

Above $\sigma_1^c = 0.726$: $u_1 = 1/b_{11} = 1/1.284 = 0.779$, $k_{11} = \exp(-b_{01}/b_{11}) = \exp(14.676/1.284) = 92{,}033$ and $Q^{**}_{c1} = b_{21} = 208{,}855$ J mol^{-1}:

$$\sigma/\sigma_{TS} = \exp\{92{,}033[t_f \exp(208{,}855/RT)]^{0.779}\} \quad (10b)$$

The validity of deriving the Wilshire failure time equation from the Wilshire minimum creep rate equation by using the Monkman-Grant relation in Eq. (2c) can be found by comparing the direct estimates of u_j and k_{1j} shown in Eqs. (10a,b) above with those implied by the Monkman- Grant relation – namely $u_j = -v_j/\rho$, $k_{1j} = k_{2j}M^{vj/\rho}$ and $Q_{cj}^{**} = \rho Q_{cj}^{*}$. So above $\sigma_1^c = 0.726$, $u_1 = -v_1/\rho = -0.708/-0.765 = 0.925$, $k_{11} = (19495)1.557^{0.925} = 29{,}362$ and $Q_{c1}^{**} = 0.765(223) = 171$ kJ mol^{-1}. Compared to the values in Eq. (10b), reasonable agreement exists only for u_1. Then below $\sigma_1^c = 0.726$, $u_2 = -v_2/\rho = -0.189/-0.765 = 0.247$, $k_{12} = (-5.958)1.557^{0.247} = 6.647$ and $Q_{c2}^{**} = -0.765(238) = 182$ kJ mol^{-1}. Compared to the values in Eq. (10a), reasonable agreement exists only for k_{12} and very good agreement only with u_2. The disparities suggest that the link between the Wilshire equations for failure times and minimum creep rates may be a different relation to the Monkman– Grant relation or modifications of it.

This Wilshire equation is visualised in Fig. 3a where on the horizontal axis the failure times are temperature compensated using the estimated activation energies. The performance of the Wilshire equation is seen by the suitability of the best fit line that is kinked at the break point defined by a normalised stress of 0.726. Alternatively, in Fig. 3b, $\ln[-\ln(\sigma/\sigma_{TS})]$ is plotted against the actual and the models predicted times to failure. The log of the time to failure is shown so that the length of the error bars (shown as dashed bars in this figure) then corresponds to the percentage prediction error (divided by 100). The predictions shown by the discontinuous solid lines give a good fit to the actual failure times.

Fig. 3 - (a) Dependence of $\ln[t_f \exp(-Q^{**}_c/RT)]$ on $\ln[-\ln(\sigma/\sigma_{TS})]$ at all temperatures; (b) Dependence of $\ln[t_f]$ on $\ln[-\ln(\sigma/\sigma_{TS})]$ with error bars equal to the % prediction error/100.

The accuracy of these predictions is further revealed in Table 2b. When the percentage errors shown by the length of the error bars in Fig, 3b are squared and then averaged, the Wilshire model predicts with a 20.78% MSPE or with a root mean percentage squared error of 45.59%. This is put into further context by noting that Theil's U is 0.019, which is scaled to be within the range of 0 to 1, with zero corresponding to a model that produced perfect predictions. Therefore, it appears that the Wilshire model is much more successful at predicting failure times compared to minimum creep rates. Based on Theil's decomposition of this MSPE, it is clear that nearly all of this error is random in nature (100%) so that the Wilshire model exhibits very little systematic error. This is further confirmed by Peel's decomposition where the p-values on α_0 a4nd α_1 in Eq. (8a) reveal that α_0 is not significantly different from zero and α_1 is not significantly different from unity so that all the percentage prediction errors are random in nature- whose magnitude is summarised in the standard deviation of e in Eq. (8a), $\sigma_e = 0.472$. Using Eq. (8f), $\exp(0.5\sigma^2_e)-1 = 11.78\%$ which is an estimate of the mean percentage prediction error assuming normality of e (this is close to the actual mean percentage prediction error of 10.22%). What is important to realise is that this average percentage error produced by the Wilshire model is all random in nature suggesting the model is not mis specified in any way and that this mean percentage error reflects the natural variation present in measuring the times to failure from experimental creep curves (and so it is unlikely that this magnitude or error can be further reduced through use of any other creep model).

Table 2b
Summary of the predictive accuracy of Eq. (2g) using the parameter estimates shown in Table 2a.

5.3. The time to various strains

Using the method of estimation given in sub section 3.3, Table 3a shows the parameter estimates of Eq. (3c) using as an example a normalised strain of $\varepsilon^* = 0.1$.

Table 3a
Least Squares Estimates of the Parameters of Eq. (3c) when $\varepsilon^* = 0.1$.

The p-value associated with d_4 in Eq. (3c) is 0.209%, suggesting that Q^{***}_c (and thus the activation energies) above and below a normalised stress of 0.726 are significantly different from each other at the 1% significance level. The p-value associated with d_3 is 9.85E-07% suggesting that the values for w^* above and below a normalised stress of 0.726 are significantly different from each other at the 1% significance level. This model is capable of explaining 96.91% of the variation observed in the logarithm of the times to a normalised strain of 0.1 (as given by the coefficient of determination, R^2). Using the estimates in Table 3a and Eq. (3c) above,

Below $\sigma_1^c = 0.726$: $w^*_2 = 1/d_{12} = 1/4.815 = 0.208$, $k^*_{32} = \exp(-d_{02}/d_{12}) = \exp(-6.118/4.815) = 0.281$ and $Q^{***}_{c2} = d_{22} = 154{,}466$ J mol^{-1}:

$$\sigma/\sigma_{TS} = \exp\{0.281[t_{\varepsilon^*}\exp(154{,}466/RT)]^{0.208}\} \quad (11a)$$

Above $\sigma_1^c = 0.726$: $w^*_1 = 1/d_{11} = 1/1.382 = 0.724$, $k^*_{31} = \exp(-d_{01}/d_{11}) = \exp(-10.021/1.382) = 0.001$ and $Q^{***}_{c1} = -d_{21} = 164{,}894$ J mol^{-1}:

$$\sigma/\sigma_{TS} = \exp\{0.001[t_{\varepsilon^*}\exp(164{,}894/RT)]^{0.724}\} \quad (11b)$$

This Wilshire model visualised in Fig. 4a where on the horizontal axis the times to a normalised strain of 0.1 are temperature compensated using the estimated activation energies. The performance of the Wilshire equation is seen by the suitability of the best fit line that is kinked at the break point defined by a normalised stress of 0.726. Alternatively, in Fig. 4b, $\ln[-\ln(\sigma/\sigma_{TS})]$ is plotted against the actual and the models predicted times to normalised strains of 0.1. The log of these times are shown so that the length of the error bars (shown as dashed bars in this figure) then corresponds to the percentage prediction error (divided by 100). The predictions shown by the discontinuous solid lines give a good fit to the actual times to normalised strains of 0.1. Equally good fits were obtained at other normalised strains.

Fig. 4- (a) Dependence of $\ln[t_{\varepsilon^*=0.1}\exp(-Q^{***}_c/RT)]$ on $\ln[-\ln(\sigma/\sigma_{TS})]$ at all temperatures; (b) Dependence of $\ln[t_{\varepsilon^*=0.1}]$ on $\ln[-\ln(\sigma/\sigma_{TS})]$ with error bars equal to the % prediction error/100.

The accuracy of these predictions is further revealed in Table 3b. When the percentage errors shown by the length of the error bars in Fig. 4b are squared and then averaged, the Wilshire model predicts with a 28.37% MSPE or with a root mean percentage squared error of 53.27%. This is put into further context by noting that Theil's U is 0.026, which is scaled to be within the range of 0 to 1, with zero corresponding to a model that produced perfect predictions. It therefore appears that the Wilshire model is much more successful at predicting times to a normalised strain of 0.1 compared to minimum creep rates, but not as successful as predicting times to failure. Based on Theil's decomposition of this MSPE, it is clear that nearly all of this error is random in nature (100%) so that the Wilshire model exhibits very little systematic error. This is further confirmed by Peel's decomposition where the p-values on α_0 and α_1 in Eq. (8a) reveal that α_0 is not significantly different from zero and α_1 is not significantly different from unity so that all the percentage prediction error is random in nature- whose magnitude is summarised in the standard deviation of e in Eq. (8a), $\sigma_e = 0.552$. Using Eq. (8f), $\exp(0.5\sigma^2_e) - 1 = 16.46\%$ which is an estimate of the mean percentage prediction error assuming normality of e (this is close to the actual mean percentage prediction error of 13.51%). What is important to realise is that this average percentage error produced by the Wilshire model is all random in nature suggesting the model is not mis specified in any way and that this mean percentage error reflects the natural variation present in measuring the times to various strains from experimental creep curves (and so it is unlikely that this magnitude or error can be further reduced through use of any other creep model).

Table 3b
Summary of the predictive accuracy of Eq. (3c) using the parameter estimates shown in Table 3a with $\varepsilon^* = 0.1$.

Fig. 5 summarise the results from estimating the parameters of Eq. ([3c) at all other normalised strains – from 0 to 1 in increments of 0.01. It can be seen that well defined relationships exists between the three Wilshire parameters and the normalised strain. In Fig. 5a it can be seen that k^*_{3j} increases in a non linear fashion with the normalised strain but this functional relationship is different above and below the break point of σ^*_c. Unsurprisingly this

is then reflected in different parameter estimates of Eqs. (6a,b) as shown in Table 4. These parameter estimates produce the predicted curves (solid curves) shown in Fig. 5a and as can be seen, the ANN produces a very good fit. Also notice that the k^*_{3j} obtained at each strain converge on the k_{1j} of the failure time equation given by Eq. (2a) as the normalised strain tends to 1. As k^*_{3j} is a combination of both d_{0j} and d_{1j} in Eq. (3c), with d_{1j} just being the inverse of w_{*j}, Fig. 5d shows the variation of just the d_{0j} with the normalised strain. Whilst the relationship is again non linear, it appears much simpler in nature than that for the k^*_{3j}.

In Fig. 5b, a more complicated relationship exists between the w^*_{3j} and the normalised strain. Below the break point of σ^*_c the relationship looks exponential in nature, but above the break it is more U shaped. Again, this is then reflected in different parameter estimates of Eqs. (6a,b) as shown in Table 4. These parameter estimates produce the predicted curves (solid curves) shown in Figure 5b and as can be seen the ANN again produces a very good fit. Also notice that the w^*_{3j} obtained at each strain converge on the u_j of the failure time equation given by Eq. (2a) as the normalised strain tends to 1. In Fig. 5c the values of Q^{***}_c and therefore the activation energies appear to depend strongly on the normalised strain but in a fashion that is very similar above and below the break point of σ^*_c. The difference in the Q^{***}_c values each side of this break point diminishes with the normalised strain but again the Q^{***}_c values obtained at each strain converge on the Q^{**}_c values of the failure time equation given by Eq. (2a) as the normalised strain tends to 1. The shape of the curves in Fig.5c are consistent with the work of Estrin and Mecking [24] with Q^{**}_c being viewed as the activation energy for steady state or minimum creep.

Fig. 5- Variations of the Wilshire parameters with the normalised strain.

Table 4
Parameter estimates of Eq. (6a) and Eq. (6b).

5.4. Individual creep curves

Table 3b only shows the performance of the Wilshire equation at a normalised strain of 0.1, but to assess its full performance this analysis should be repeated for all normalised strains. That is, the ability of the Wilshire equation to predict full creep curves is required. Table 5 summarises the results of such analysis. This involved the following steps: 1. Insert the parameters estimates shown in Table 4 into Eqs. (6) to predict the Wilshire parameters k^*_{3j}, w^*_j and Q_{cj}^{***} at all normalised strains ε^*. 2. Insert these predicted values for the parameters k^*_{3j}, w^*_j and Q_{cj}^{***}, together with all the stress and temperatures in the experimental data set into Eq. (3f) to predict the time to all these strains at all these stresses and temperatures. 3. Compare the predicted times along the creep curves to the experimentally measured ones by converting the normalised strains back to actual strains and apply Eqs. (7c,d,e) and Eq. (8e) to assess how close the predicted and experimental creep curves are. This involves a comparison of 30 experimental creep curves with their predicted counterparts using the Wilshire equation.

Table 5
Summary of the predictive accuracy of Eq. (3f) using the parameter estimates shown in table 4 and all the experimental stress and temperature test conditions.

The Wilshire model predicts the experimental creep curves with a 49.54% MSPE or with a root mean percentage error of 70.4%. This is put into further context by noting that

Theil's U is 0.03, which is scaled to be within the range of 0 to 1, with zero corresponding to a model that produced perfect predictions. Based on Theil's decomposition of this MSPE, it is clear that nearly all of this error is random in nature (98.51%) so that the Wilshire model exhibits very little systematic error. This is further confirmed by Peel's decomposition where the p-values on α_0 and α_1 in Eq.(8a) reveal that α_0 is not significantly different from zero and α_1 is not significantly different from unity so that all the percentage prediction error is random in nature- whose magnitude is summarised in the standard deviation of e in Eq. (8a), $\sigma_e = 0.70$. Using Eq. (8f), $\exp(0.5\sigma^2_e) - 1 = 27.76\%$ which is an estimate of the mean percentage difference between the predicted and experimental creep curves assuming normality of e.

Whilst Table 5 provides a good summary of the overall predictive accuracy, it is useful to visualise this accuracy in a series of figures. This Fig. 6 plots the MSPE associated with each of the 30 creep curves making up the experimental data set. The average error over all test conditions is of course 49.54% but there are big disparities across all the experimental test conditions. The predicted creep curves at 923K are closest to the experimental creep curves where the MSPE is never more than 45% over the different stresses. The biggest discrepancies between actual and predicted creep curves occur at 873K and 200 MPa and again at 973K at 700 and 950 MPa. But the Wilshire equation predicts creep curves with a MSPE below 50% over the vast majority of test conditions.

Fig. 6 - Creep curve predictive accuracy at differing test conditions as measured by the MSPE.

Fig. 7 - Experimental and predicted creep curves at four different illustrative test conditions; a. 973K and 200 MPa; b. 923K and 870 MPa; c. 1023K and 500 MPa; d. 873K and 950 MPa;

Finally, Figures 7 show some test conditions corresponding to worst and best predictions made for the experimental creep curves. In Figs. 7a and 7c, which visualise the worst performing test conditions, the creep curves shape is well predicted but there is consistent over prediction of the time to failure. Where this occurs at other test conditions, the predictions are often under predictions and this explains the low value for U^M and high value for U^C in Table 5. In Figs. 7b and 7d, which visualise some of the best performing test conditions, the creep curves shape is well predicted in the primary/secondary stages of creep but not so much in the tertiary stages. However, over all stages there is no tendency to under or over predict. These two figures are typical of all the test conditions with a low MSPE (further figures are available from the author upon request).

6. Conclusion

This paper introduced an artificial neural network (ANN) methodology for extending the Wilshire Equation related to times to specified strains so that complete creep curves can be predicted at any test conditions (including operating conditions) using just accelerated test data. The paper also presented various statistics for the evaluation of predictions made by the this modified Wilshire model. These statistics also provide a suitable way of comparing different creep prediction models as they are scaled values and so should prove useful in future research on creep prediction. When these techniques and predictions were applied to Waspaloy the following conclusions could be drawn:

1. There is a small but statistically significant change in the activation energy for Waspaloy at a normalised stress of 0.72. The original Wilshire paper failed to identify the break occurring at this normalised stress. This change in activation energy is also smaller than that observed by Whittaker et. al. but could be due (as they state) to the amount of strain hardening in an alloy brought about by high dislocation densities generated at stresses above a normalised stress of 0.726.

2. Using the Wilshire time to strain equation expressed in normalised strain space, it was possible to measure the activation energy and various different strains and the results support the work of Estrin and Mecking [24] who proposed that the activation energy would be dependant on strain in the way seen in this paper.

3. The Wilshire equations for minimum creep rates and failure times produce very good predictions, with U values very close to zero and with mean squared percentage errors of 45% and 20% respectively.

4. The Monkman-Gant relation does not provide a completely satisfactory link between the Wilshire minimum creep rate and time to failure equations.

5. The parameters of the Wilshire time to strain equation have a well defined and systematic relationship with the normalised strain and these functional relationships are extremely well model by a simple artificial neural network (ANN). Because the parameters tend in value to those of the Wilshire time to failure equation as the normalised strain tends to 1, the predicted creep curves are well behaved in that they do not "curve back on themselves" at high strains.

6. When the ANN is combined with the Wilshire equation for times to strains, the creep curves as not as accurately predicted as the end points of the curve (failure times) or the minimum creep rate associated with the curve – the mean squared percentage errors is 49%. That said, the model works well at predicting creep curves with a U value of 0.03 and for most test conditions present in the experimental data set used for this paper, the predicted creep curves were in very close agreement with the experimental curves with mean squared percentage errors less than 20%.

Important areas for future research include the application of the evaluation statistics given in this paper to other aero engine materials (e.g. RR1000) and perhaps more importantly to use these statistics to compare other creep curve prediction techniques (such that given by Eqs. [5]) with the Wilshire equation so as to rank the techniques in terms of their accuracy.

References

[1] P. Ruffles: *Aerospace Structural Materials: Present and Future*, The Institute of Materials, London, 1995.

[2] Materials UK Energy Review: Report 1, Energy Materials – Strategic Research Agenda, 2007.

[3] B. Wilshire and A. J. Battenbough: Creep and creep fracture of polycrystalline copper. *Materials Science and Engineering A*, 2007, 443, pp. 156-166.

[4] B. Wilshire and P. J. Scharning: Prediction of long term creep data for forged 1Cr-1Mo-0.25V steel. *Materials Science and Technology*, 2008, 24(1), pp. 1-9.

[5]. B. Wilshire, and M. Whittaker: Long term creep life prediction for Grade 22 (2·25Cr—1Mo) steels. *Materials Science and Technology*, 2011, 27(3), pp. 642-647.

[6] M. Evans: Incorporating specific batch characteristics such as chemistry, heat treatment, hardness and grain size into the Wilshire equations for safe life prediction in high temperature applications: An application to 12Cr stainless steel bars for turbine blades. *Applied Mathematical Modelling*, 2016, 40(23-24), pp. 10342-10359.

[7] B. Wilshire and P. J. Scharning: A new methodology for analysis of creep and creep fracture data for 9–12% chromium steels. *International Materials Reviews*, 2008, 53(2), pp. 91-104.

[8] M. T. Whittaker, M. Evans and B. Wilshire: Long-term creep data prediction for type 316H stainless steel. *Materials Science and Engineering A*, 2012, 552, pp. 145-150.

[9] M. T. Whittaker, W. Harrison, C. Den , C. Rae and S. Williams: Creep Deformation by Dislocation Movement in Waspaloy. *Materials*, 2017, 10(1), pp. 61.

[10] B. Wilshire B and P. J. Scharning: Extrapolation of creep life data for 1Cr-0.5Mo Steel. *Int. J. Press. Vessel. Pip*., 2008, 85, pp. 739–743.

[11] M. T. Whittaker, W. J. Harrison, R.J. Lancaster and S. Williams: An analysis of modern creep lifing methodologies in the Titanium alloy Ti6-4, *Mater. Sci. Eng. A*, 2013, 577, pp. 114–119.

[12] W. Harrison, M. T. Whittaker and S. Williams: Recent Advances in Creep Modelling of the Nickel Base Superalloy, Alloy 720Li. *Materials*. 2013, 6, pp. 1118–1137.

[13] Z. Abdallaha, K. Perkins and S. Williams: Advances in the Wilshire extrapolation technique—Full creep curve representation for the aerospace alloy Titanium 834, *Materials Science and Engineering: A*, 2012, 550(30), pp. 176-182.

[14] V. Gray and M .T. Whittaker: Development and Assessment of a New Empirical Model for Predicting Full Creep Curves, *Materials*, 2015, 8, pp. 4582-4592.

[15] R. W. Evans and B. Wilshire: *Creep of Metals and Alloys*, The Institute of Metals, London, 1985.

[16] B. Wilshire B and P. J. Scharning: Theoretical and practical approaches to creep of Waspaloy. *Materials Science and Technology*, 2009, 25(2), pp. 242-248.

[17]. F.C. Monkman and N. J. Grant: An empirical relationship between rupture life and minimum creep rate in creep-rupture tests. *Proc. ASTM.*, 1956, 56, pp. 593–620.

[18] D. C. Dunand, B.Q. Han and A.M. Jansen: Monkman-Grant analysis of creep fracture in dispersion-strengthened and particulate-reinforced aluminium, *Metallurgical and Materials Transactions A*, 1999, 30(13), pp. 829-838.

[19] National Institute for Materials Science (NIMS), Data Sheets on Elevated Temperature Properties, Tokyo, Japan, various Creep Data Sheets and Years.

[20] ECCC Recommendations, Creep Data Validation and Assessment Procedures, www.ommi.co.uk/etd/eccc/open.htm, 2005, Vols. 1–9.

[21] High Temperature Properties of Steels, Proceedings of the Joint Conference organised by the British Iron & Steel Research Association and the Iron and Steel Institute, Eastbourne, 1966.

[22] V. C. Martin, S. Hurn and D. Harris: *Econometric Modelling with Time Series: Specification, Estimation and Testing*, Cambridge University Press, Cambridge, 2013.

[23] R. G. Davies: On the activation energy of high temperature creep, *Acta Metallurgica*, 1961, 9, 1035-1036.

[24] Y. Estrin and H. Mecking: A unified phenomenological description of work hardening and creep based on one-parameter models, *Acta Metallurgica*, 1984, 32(1), 57-70.

[25] H. Akaike: On Entropy Maximisation Principle, in P. R. Krishniah (ed.), *Applications of Statistics*, Amsterdam, North Holland, 1977.

[26] H. Theil: *Applied Economic Forecasts*, Amsterdam, North Holland, 1966.

[27] K. Holden, D.A. Peel, and J. L Thompson: *Economic Forecasting: An Introduction*, Cambridge University Press, Cambridge, 1990.

Table 1a

Least Squares Estimates of the Parameters of Eq. (1b) with p = 2.

	Above $\sigma_1^c = 0.726$			Below $\sigma_1^c = 0.726$		
Parameters	a_{01}	a_{11}	a_{21}	a_{02}	a_{12}	a_{22}
Estimate	13.958	-1.413	-223,374	9.508	-5.328	-237,586
Standard error	2.744	0.332	20,841	2.811	0.630	3,565
p-value	0.002	0.023	0.000	0.220	0.000	0.000

The p–value gives the probability (in %) of the null hypothesis being true, where the null hypothesis is that the model parameter equals zero. An p–value below α% therefore indicates a parameter (and thus test variable) that is statistically significant at the α% significance level.

Table 1b

Summary of the predictive accuracy of Eq. (1b) using the parameter estimates shown in Table 1a.

Theil's Decomposition		Peel's Decomposition			
U^M	0.00%	U^M	0.00%	α	0.000 [1]
U^S	0.00%	U^R	0.94%	β	1.000[1]
U^C	100.00%	U^D	99.06%	R^2	96.30%
U	0.022	-	-	σ_e	0.700
MSPE	45.61%	-	-	-	-

p-values associated with the null hypothesis that $\alpha_0 = 0$ and $\alpha_1 = 1$ are shown in parenthesis and assume that the random error term e in Eq. (8a) is normally distributed. The U decompositions are defined by Eqs. (7c,d,e) and Eq. (8e). α_0 and α_1 are the least squares estimates of the parameters in Eq. (8a) and σ_e is the estimated standard deviation for e. R^2 is the percentage variation in $\ln[y_i^a]$ explained by $\ln[y_i^b]$ in Eq. (8a).

Table 2a

Least Squares Estimates of the Parameters of Eq. (2g).

	Above $\sigma_1^c = 0.726$			Below $\sigma_1^c = 0.726$		
Parameters	b_{01}	b_{11}	b_{21}	b_{02}	b_{12}	b_{22}
Estimate	-14.676	1.284	208,855	-11.368	4.194	217,857
Standard error	1.852	0.224	14,068	1.852	0.425	2,406
p-value	0.000	0.0001	0.000	0.0002	0.000	0.000

The p–value gives the probability (in %) of the null hypothesis being true, where the null hypothesis is that the model parameter equals zero. An p–value below α% therefore indicates a parameter (and thus test variable) that is statistically significant at the α% significance level.

Table 2b

Summary of the predictive accuracy of Eq. (2g) using the parameter estimates shown in Table 2a.

Theil's Decomposition		Peel's Decomposition			
U^M	0.00%	U^M	0.00%	α	0.000 [1]
U^S	0.00%	U^R	0.71%	β	1.000[1]
U^C	100.00%	U^D	99.29%	R^2	97.20%
|U	0.019	-	-	σ_e	0.472
MSPE	20.78%	-	-	-	-

p-values associated with the null hypothesis that $\alpha_0 = 0$ and $\alpha_1 = 1$ are shown in parenthesis and assume that the random error term e in Eq. (8a) is normally distributed. The U decompositions are defined by Eqs. (7c,d,e) and Eq. (8e). α_0 and α_1 are the least squares estimates of the parameters in Eq. (8a) and σ_e is the estimated standard deviation for e. R^2 is the percentage variation in $\ln[y_i^a]$ explained by $\ln[y_i^b]$ in Eq. (8a).

Table 3a

Least squares estimates of the parameters of Eq. (3c) when $\varepsilon^* = 0.1$.

	Above $\sigma_1^c = 0.726$			Below $\sigma_1^c = 0.726$		
Parameters	d_{01}	d_{11}	d_{21}	d_{02}	d_{12}	d_{22}
Estimate	-10.021	1.382	154,894	-6.118	4.815	164,466
Standard error	2.164	0.262	16,437	2.164	0.497	2,812
p-value	0.008	0.001	0.000	0.87	0	0

The p–value gives the probability (in %) of the null hypothesis being true, where the null hypothesis is that the model parameter equals zero. An p–value below α% therefore indicates a parameter (and thus test variable) that is statistically significant at the α% significance level.

Table 3b

Summary of the predictive accuracy of Eq. (3c) using the parameter estimates shown in Table 3a with $\varepsilon^* = 0.1$.

Theil's Decomposition		Peel's Decomposition			
U^M	0.00%	U^M	0.00%	α	0.000 [1]
U^S	0.00%	U^R	0.78%	β	1.000[1]
U^C	100.00%	U^D	99.22%	R^2	96.91%
U	0.026	-	-	σ_e	0.552
MSPE	28.37%	-	-	-	-

p-values associated with the null hypothesis that $\alpha_0 = 0$ and $\alpha_1 = 1$ are shown in parenthesis and assume that the random error term e in Eq. (8a) is normally distributed. The U decompositions are defined by Eqs. (7c,d,e) and Eq. (8e). α_0 and α_1 are the least squares estimates of the parameters in Eq. (8a) and σ_e is the estimated standard deviation for e. R^2 is the percentage variation in $\ln[y_i^a]$ explained by $\ln[y_i^b]$ in Eq. (8a).

Table 4
Parameter estimates of Eq. (6a) and Eq. (6b).

	Above σ^c_1				
	w^*_1		k^*_{31}		Q^{***}_{c1}
δ_{011}	322.778	δ_{211}	324.293	δ_{411}	322.779
δ_{111}	7.868	δ_{311}	-2.126	δ_{511}	97.106
δ_{021}	31.532	δ_{221}	31.52	δ_{421}	31.532
δ_{121}	7.863	δ_{321}	-2.126	δ_{521}	13.636
β_{11}	1.1E+142	λ_{11}	5.2E+149	γ_{11}	-5E+142
β_{21}	-3.7E+15	λ_{21}	-3.7E+22	γ_{21}	-5.1E+15
ϕ_{01}	0.234	ϕ_{21}	-87991.1	ϕ_{41}	184.577
ϕ_{11}	0.005	ϕ_{31}	-120281	ϕ_{51}	35.538
	Below σ^c_1				
	w^*_2		k^*_{32}		Q^{***}_{c2}
δ_{012}	322.779	δ_{212}	324.293	δ_{412}	322.779
δ_{112}	42.422	δ_{312}	15.438	δ_{512}	92.977
δ_{022}	31.532	δ_{222}	31.52	δ_{422}	31.532
δ_{122}	3.098	δ_{322}	-5.044	δ_{522}	12.911
β_{12}	-4E+139	λ_{12}	-3E+141	γ_{12}	-4E+142
β_{22}	-6.7E+12	λ_{22}	-5.6E+11	γ_{22}	-4.6E+15
ϕ_{02}	0.829	ϕ_{22}	2.954	ϕ_{42}	173.938
ϕ_{12}	-0.044	ϕ_{32}	13.828	ϕ_{52}	37.345

Table 5
Summary of the predictive accuracy of Eq. (3f) using the parameter estimates shown in table 4 and all the experimental stress and temperature test conditions.

Theil's Decomposition		Peel's Decomposition			
U^M	0.34%	U^M	0.34%	α	-0.015 [0.76]
$U^{S\&}$	1.15%	U^R	0.10%	β	0.998 [0.59]
U^C	98.51%	U^D	99.65%	R^2	94.66%
U	0.030	-	-	σ_e	0.700
MSPE	49.54%	-	-	-	-

p-values associated with the null hypothesis that $\alpha_0 = 0$ and $\alpha_1 = 1$ are shown in parenthesis and assume that the random error term e in Eq. (8a) is normally distributed. The U decompositions are defined by Eqs. (7c,d,e) and Eq. (8e). α_0 and α_1 are the least squares estimates of the parameters in Eq. (8a) and σ_e is the estimated standard deviation for e. R^2 is the percentage variation in $\ln[y_i^a]$ explained by $\ln[y_i^b]$ in Eq. (8a).

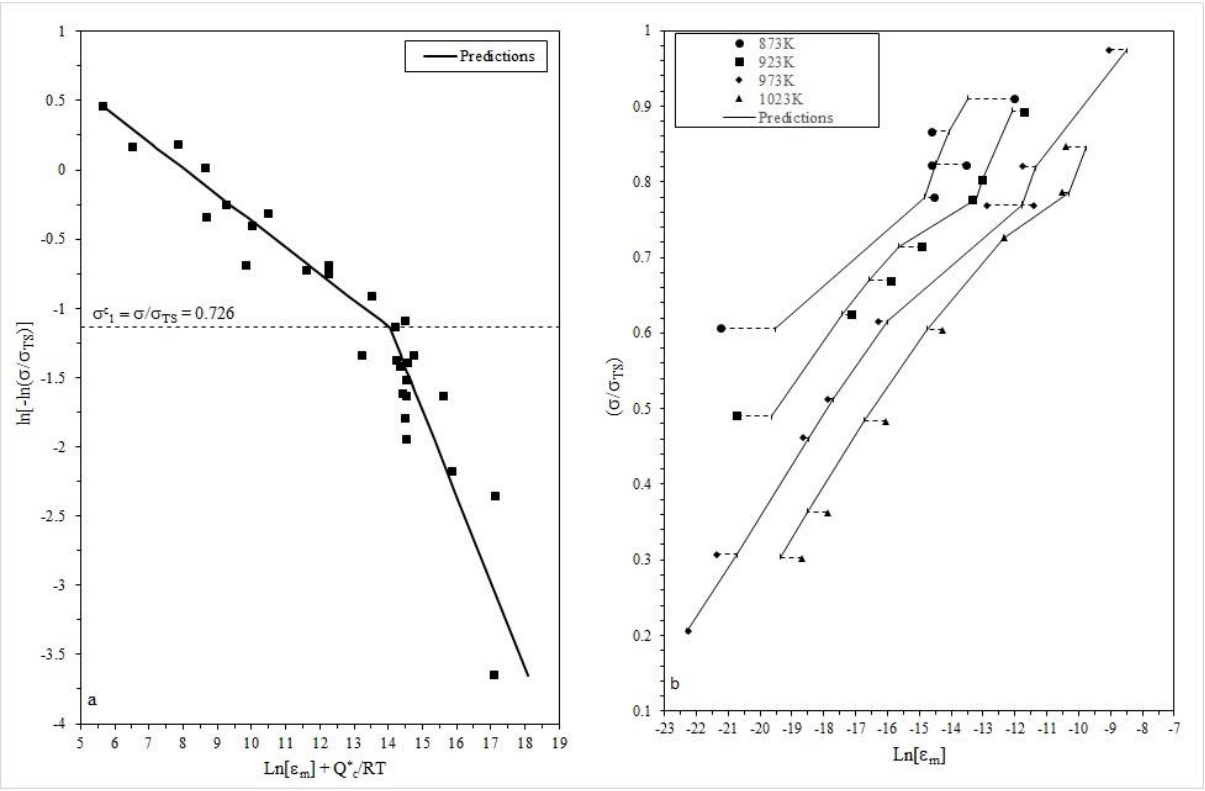

Fig. 1 - (a) Dependence of $\ln[\dot{\varepsilon}_m \exp(Q^*_c/RT)]$ on $\ln[-\ln(\sigma/\sigma_{TS})]$ at all temperatures; (b) Dependence of $\ln[\dot{\varepsilon}_m]$ on $\ln[-\ln(\sigma/\sigma_{TS})]$ with error bars equal to the % prediction error/100.

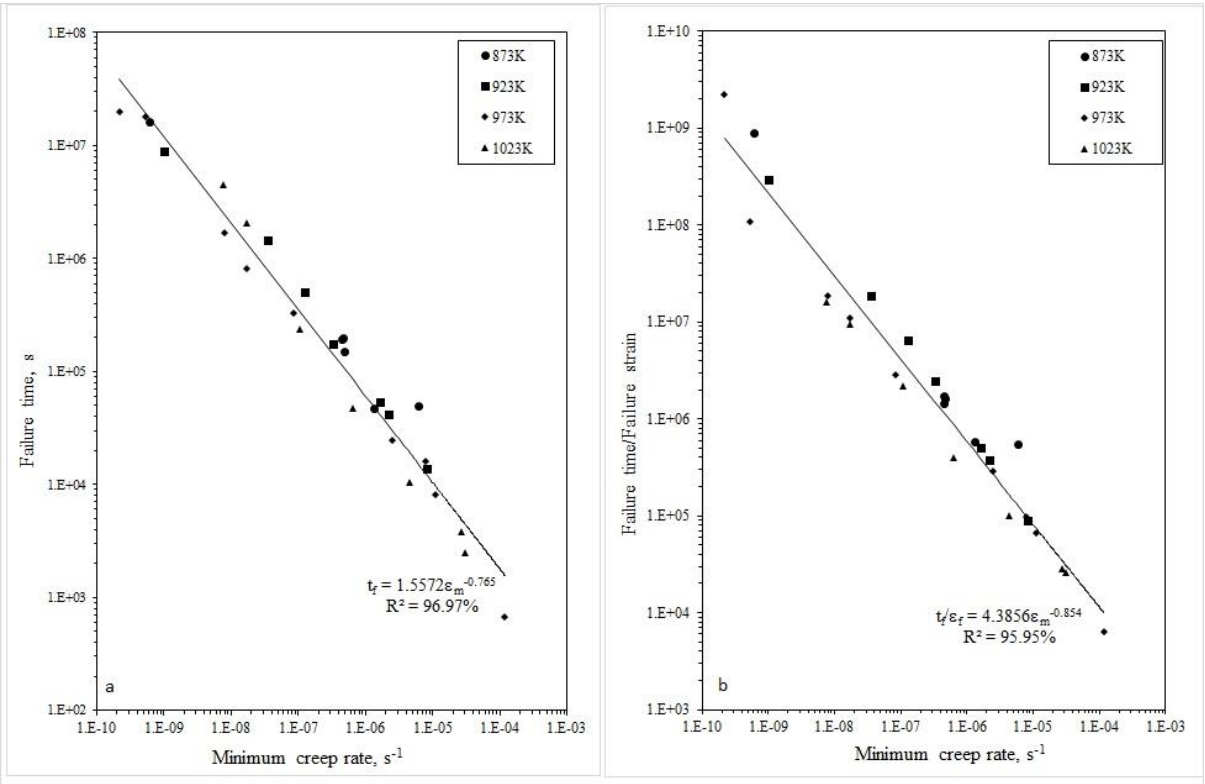

Fig. 2- (a) Dependence of $\ln[\dot{\varepsilon}]$ on $\ln[t_f]$ at all temperatures; (b) Dependence of $\ln[\dot{\varepsilon}_m]$ on $\ln[t_f] - \ln[\varepsilon_f]$.

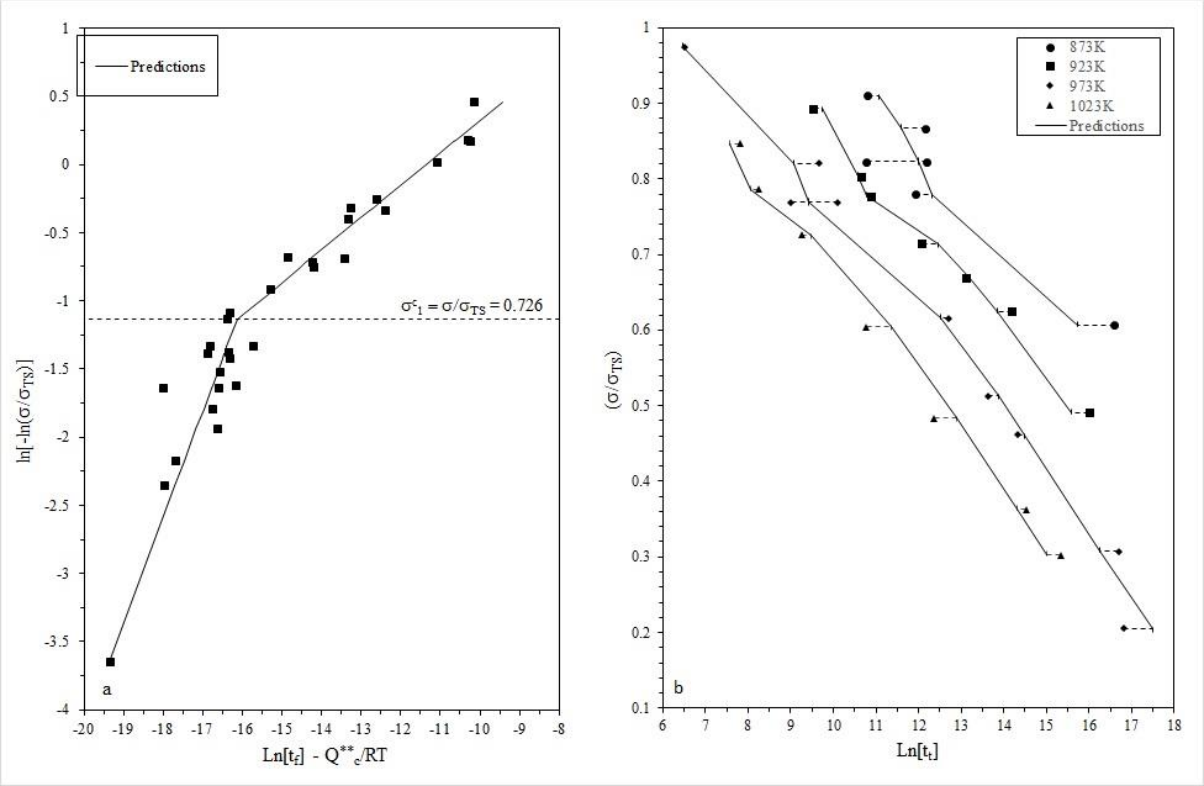

Fig. 3 - (a) Dependence of $\ln[t_f \exp(-Q^{**}_c/RT)]$ on $\ln[-\ln(\sigma/\sigma_{TS})]$ at all temperatures; (b) Dependence of $\ln[t_f]$ on $\ln[-\ln(\sigma/\sigma_{TS})]$ with error bars equal to the % prediction error/100.

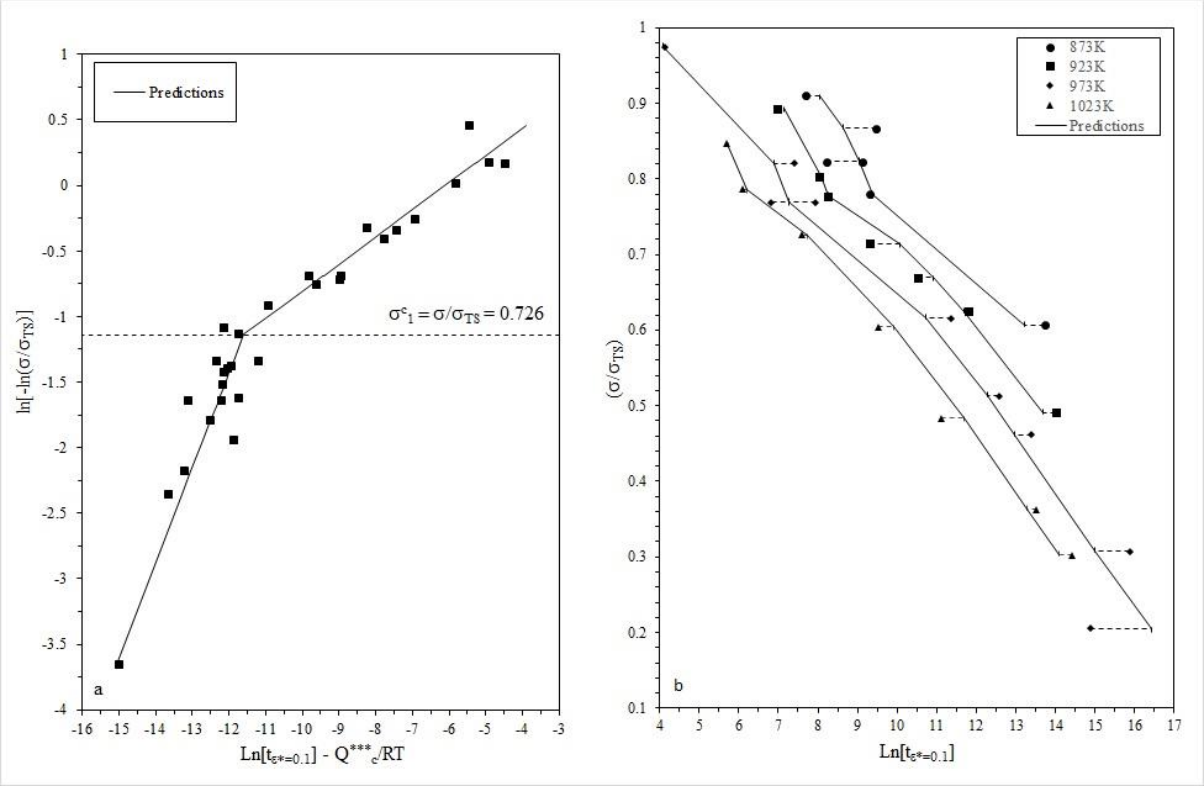

Fig. 4- (a) Dependence of $\ln[t_{\varepsilon^*=0.1}\exp(-Q^{***}_c/RT)]$ on $\ln[-\ln(\sigma/\sigma_{TS})]$ at all temperatures; (b) Dependence of $\ln[t_{\varepsilon^*=0.1}]$ on $\ln[-\ln(\sigma/\sigma_{TS})]$ with error bars equal to the % prediction error/100.

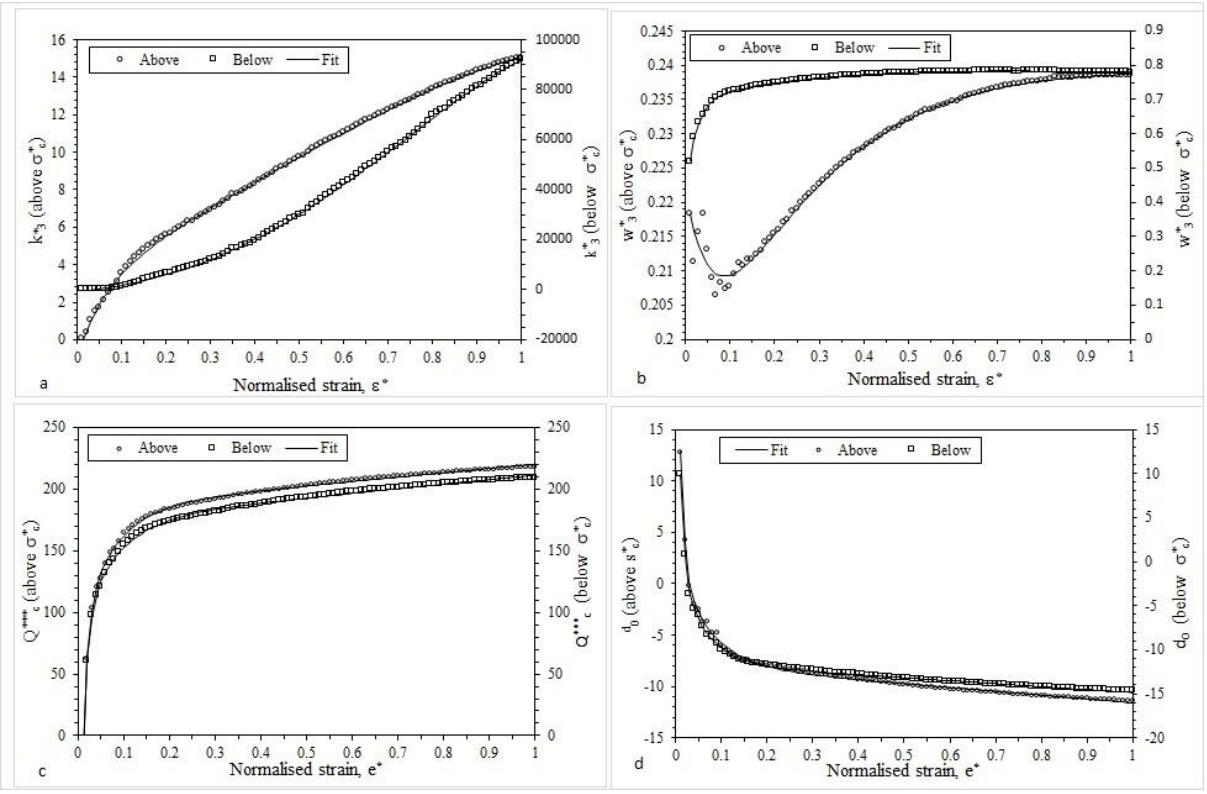

Fig. 5- Variations of the Wilshire parameters with the normalised strain.

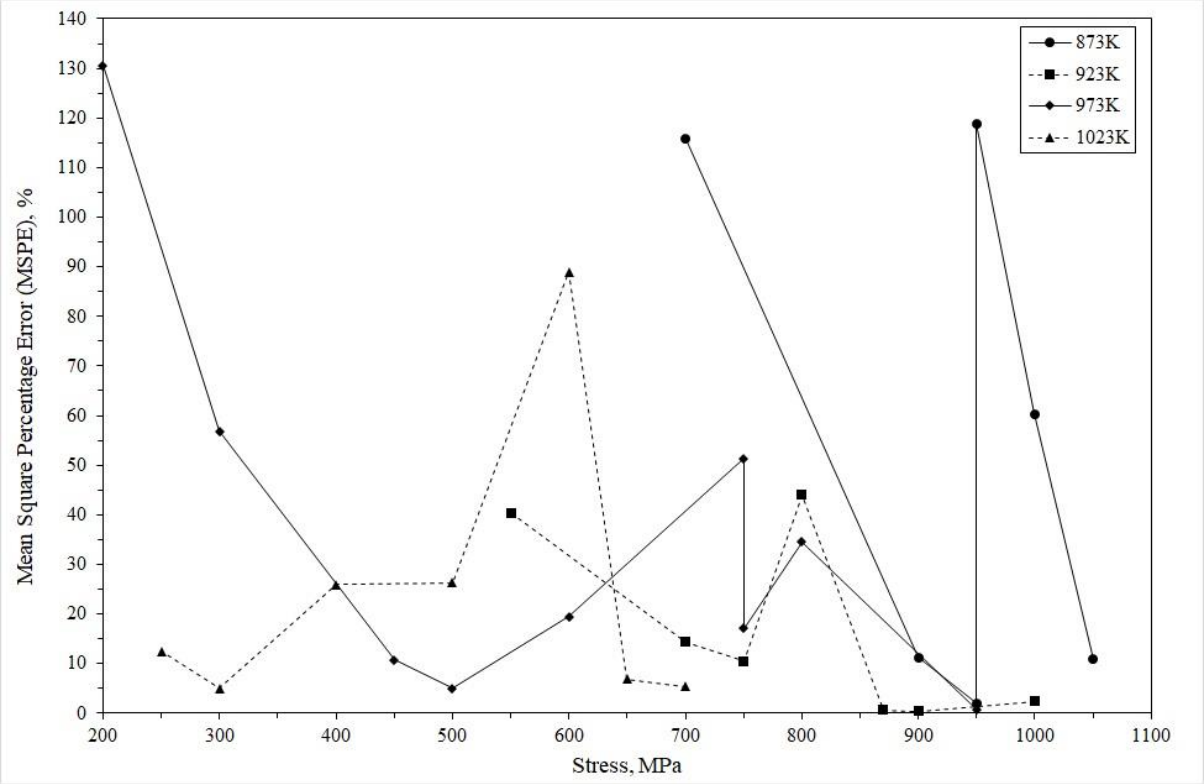

Fig. 6 - Creep curve predictive accuracy at differing test conditions as measured by the MSPE.

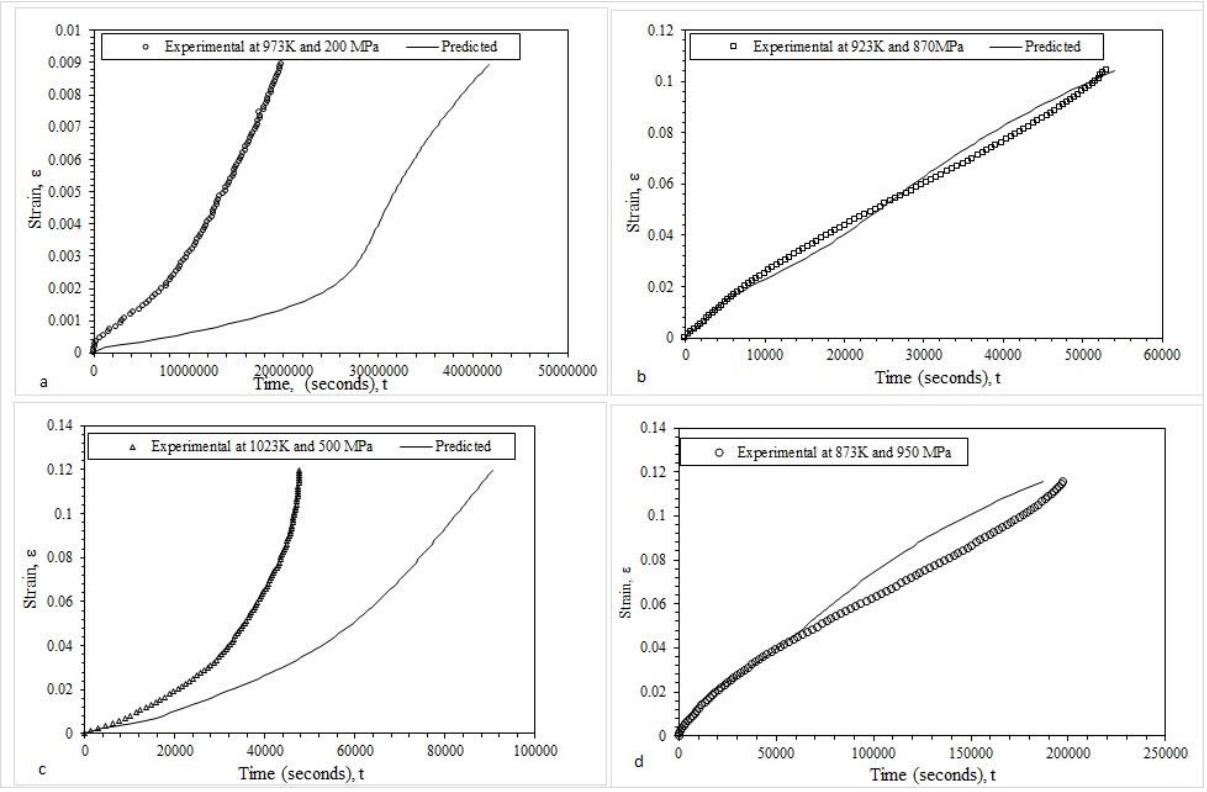

Fig. 7 - Experimental and predicted creep curves at four different illustrative test conditions; a. 973K and 200 MPa; b. 923K and 870 MPa; c. 1023K and 500 MPa; d. 873K and 950 MPa;